*Atmósfera(1997), **10**, pp. 161-178*

Photochemical box model for Mexico City

A. T. YOUNG, E. A. BETTERTON

Department of Atmospheric Sciences, University of Arizona, Tucson, Arizona, 85721

L. SALDIVAR DE RUEDA

Departamento de Química Analítica, Facultad de Química, Universidad Nacional Autónoma de México, México 04510 D.F., México

(Manuscript received May 20, 1996; accepted in final form Jan. 20, 1997)

RESUMEN

Se ha desarrollado un modelo de caja fotoquímica de multinivel para el área metropolitana de la Ciudad de México (MCMA). Se utilizó una combinación de mediciones *in situ* y estimaciones de inventarios de emisiones para obtener las estimaciones de especiación de los hidrocarburos y de las emisiones, así como de las emisiones de NO_x. Los resultados preliminares indican que ciertas estimaciones de las emisiones de NO_x pueden ser demasiado altas por un factor 2.

Esto podría hacer que las isopletas calculadas del ozono indicaran que la producción de O_3 en el MCMA podría ser limitda por los hidrocarburos. Las estrategias de control de éstos y/o del NO_x no deberían hacerse efectivas antes de que un inventario confiable de las emisiones esté disponible.

ABSTRACT

A multi-level, photochemical box model has been developed for the Mexico City metropolitan area (MCMA). A combination of *in situ* measurements and emission inventory estimates was used to obtain estimates of hydrocarbon speciation and emissions as well as NO_x emissions. Preliminary results indicate that certain emissions estimates of NO_x may be too high by a factor of two.

This could cause the calculated, ozone isopleths to indicate that atmospheric O_3 production in the MCMA could be hydrocarbon-limited. Hydrocarbon and/or NO_x control strategies should not be implemented before a reliable emissions inventory is available.

1. Introduction

With a population near 20,000,000, the Mexico City metropolitan area (MCMA) generally is recognized as one of the larger and more polluted urban centers in the world today. Concentrations of monitored "criteria" air pollutants often exceed values deemed potentially harmful. For example, ozone levels in the industrial northeastern sector of the MCMA exceeded the 0.12 parts-per-million by volume (ppmv) standard for fourteen or more days for each January through March in the years 1988 through 1991 (Coordinacion General de Reordenacion Urbana y Proteccion Ecológica, 1991). Furthermore, ozone levels often exceed the standard by 200 percent, especially in the dry season.

Measures to reduce emissions of primary pollutants have been taken, but it is difficult to determine whether these actions have resulted in significant improvement (Bravo *et al.*, 1991). A validated air pollution model is required to aid in making effective decisions on reducing pollution in the MCMA. However, few model runs for the MCMA appear to have been published in the peer-reviewed literature. Here we describe the use of a multi-level Eulerian photochemical box model to simulate air pollution in the MCMA to lay the groundwork for construction of ozone isopleths (Dunker *et al.*, 1984). Atmospheric conditions of the tropical MCMA differ substantially from most mid-latitude metropolitan areas which have been modeled in the past. Also, as recently noted by Ruiz-Suárez *et al.* (1993), the chemical mechanisms used for mid-latitude cities may not be directly applicable to Mexico City.

Although photochemical models are notoriously sensitive to initial conditions, comprehensive emissions inventories and detailed meteorological data are unavailable at present for the MCMA. In an attempt to address this problem, we sampled the urban air on two occasions and report here a partial hydrocarbon speciation for the MCMA. These measurements (described below) are insufficient for effective fine-grid or trajectory modeling of the MCMA. However, a first-order approximation of hydrocarbon speciation may be achieved.

The primary disadvantage of the box model concerns the use of averaged source concentrations and meteorology within the modeled region. The vehicle fleet in the MCMA appears to be the major source of air pollutants (Japan International Cooperation Agency (JICA)), 1988; Ruiz-Suárez, 1989). The fleet is spread fairly evenly over the entire modeled domain, although there are higher concentrations on major thoroughfares. Similarly, the meteorology of the MCMA is usually fairly uniform, with the exception of diurnal winds which can have a marked effect on pollutant distribution (Jáuregui, 1988).

Model runs used meteorological conditions of June 5, 1989, a day in the wet season, although there was no reported precipitation. There were light winds throughout the day and little cloud cover. Consequently solar radiation data were not adjusted for clouds or precipitation.

2. Geography and climate

The MCMA (19°24' N, 99°12' W) covers a flat area of about 600 km^2 and is located in the southwestern part of the Mexico Basin (Fig. 1). The valley floor is at an altitude of 2240 m above sea level. Mountains, which reach heights of 600 to 800 m above the valley floor, surround all but the northeastern part of the MCMA. The terrain slopes upward gently in this direction. The airport, located at the northeastern boundary of the city, is close to the geographical center of the Valley of Mexico.

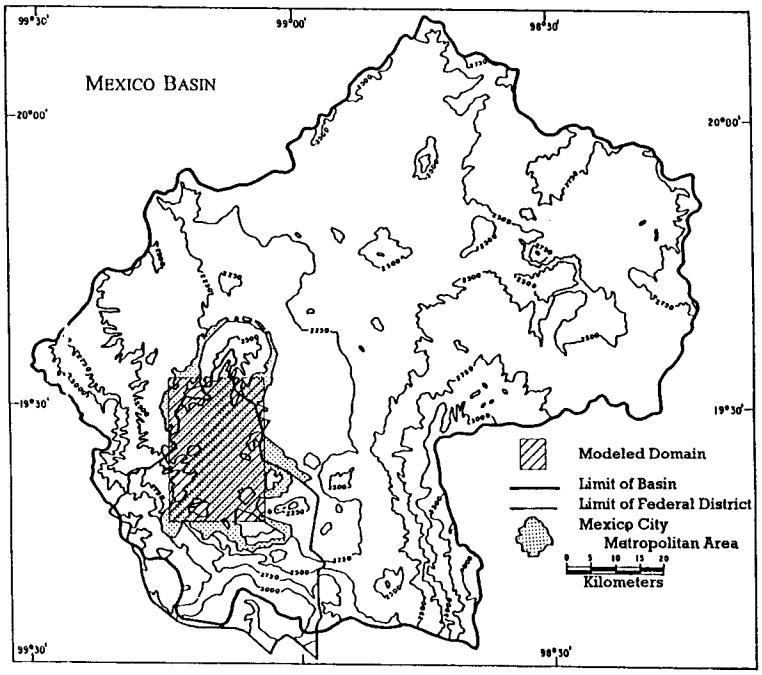

Fig. 1. Map of the Mexico city basin showing local topography and the modeled domain (Jáuregui, 1988).

The climate of the Mexico City region normally is classified according to the wet and dry seasons rather than summer and winter seasons (Jáuregui, 1988). The wet season lasts from May to September (Intergovernmental Technical Secretariat, 1991) and the city receives heavy rain from moist trade winds regularly during the months of June through September. Annual precipitation varies from 400 to 1300 mm, from east to west across the basin (Jáuregui, 1971; Jáuregui, 1973). The average relative humidity of the region is 55 to 75 percent during the wet season (JICA, 1988) but there are large variations from site to site (Jáuregui, 1971). The dry season occurs from October to April. Two synoptic-scale wind patterns exist. Anticyclonic flow from the west brings clear skies to the region from November to April. Mountain and valley winds often overcome synoptic flow in the early morning and nighttime hours during these months. During this season, skies are generally clear, mid-day winds are light, and average relative humidity can drop below 45 percent (JICA, 1988). Surface winds are generally northeasterly throughout the year.

Mean monthly temperatures in this tropical city show a small seasonal variation, but large differences may be found from site-to-site and diurnally. Monthly average surface air temperatures for the MCMA range between 12 and 18 C with the maximum occurring just before the start of the rainy season (JICA, 1988). The minimum occurs in December or January. Diurnal variations in temperature may range close to 14 C during the dry season, with smaller differences observed during the wet season (JICA, 1988). Thermal inversions occur throughout the year, but are most prevalent during the dry season. The Intergovernmental Technical Secretariat (1991) reports that for the years 1986 through 1989, the inversions existed for 20 days or more in each of the months from October through May, but only 15 days or less for the other months.

The geographical and atmospheric characteristics of the MCMA generally are conducive to trapping air

pollutants. The mountains create a bowl which inhibits ventilation of polluted air, especially when winds are light and surface inversions are present. These conditions can lead to severe pollution episodes, particularly in the dry season.

The heat island effect (Jáuregui, 1973; 1986; 1988) can enhance diurnal valley winds which can draw additional pollutants into the region at night. The combination of a lower latitude and high altitude leads to a decreased solar optical path and a higher solar intensity in the MCMA, compared to that in mid-latitude cities. The resulting enhanced photochemistry can lead to increased ozone and other secondary pollutants.

3. Model description

The Eulerian photochemical computer model used in this study is based on the model first developed at the California Institute of Technology, the CIT airshed model (Falls and Seinfeld, 1978; McRae *et al.*, 1982; McRae *et al.*, 1983; Russell *et al.*, 1988a; Russell *et al.*, 1988b; Harley *et al.*, 1993). The computer code has been revised as more accurate rate coefficients and mechanisms have become available. The model used in this study is used to calculate the concentrations of 21 chemical species using 57 differential equations that are solved using the predictor-corrector method developed by Young and Boris (1977). Computer coding was checked by running known test cases from the literature (Seinfeld, 1986). Modifications arising from characteristics specific to Mexico City (see below) were included. The chemical mechanism is summarized in Table 1, while the rate coefficients are listed in Table 2. Model runs started at 00:00 (local time) of the chosen day and lasted 24 hours.

Photochemical rate coefficients were calculated using actinic flux, solar zenith angles, species absorption cross-section, and species quantum yield (Table 3). Calculated J_{NO2} values are expected to be within 5% of those measured recently in Mexico City (Castro *et al.*, 1996). The solar data are detailed in Demerjian *et al.*, 1980. The actinic flux, corrected for surface altitude and height above surface for upper levels in the box, as a function of solar zenith angle was determined for the latitude of Mexico City. The zenith angles as a function of hour were then determined for the modeled day.

The modeled domain (Fig. 1) was set as a rectangular box centered around the Tacubaya Observatory in the west-central section of the Valley of Mexico. The floor of the box coincides with the traffic survey for narrower roads analyzed by JICA (1988). Meteorological data from that station represented first approximations of conditions within the box. The box extended vertically a total of 1100 m, with 5 horizontal layers comprising the whole box. The tops of these layers were at altitudes of 38, 154, 308, 671, and 1100 m.

Pollutants were allowed to migrate vertically between the layer boundaries. The model accounted for non-advective pollutant fluxes between layers through the K-theory hypothesis (McRae *et al.*, 1982). This hypothesis allowed closure of the continuity equation for all species.

Turbulent diffusivity causes significant mixing of pollutants within the mixing layer, and is therefore important to quantify in photochemical pollution models. Unfortunately, direct measurement of eddy diffusivities is difficult, so these quantities were calculated indirectly. Since we had limited meteorological data from the MCMA, the formulation for diffusivity was kept simple. The availability of wind speed data

TABLE 1. Chemical Mechanism Used in the Photochemical Box Model.

Reaction No.	Reaction
1.	NO2 + HV = NO + O
2.	O + O2 + M = O3 + M
3.	O3 + NO = NO2 + O2
4.	NO2 + O = NO + O2
5.	NO + O = NO2
6.	NO2 + O = NO3
7.	O3 + NO2 = NO3 + O2
8.	NO3 + NO = NO2 + NO2
9.	NO + OH = HNO2
10.	HNO2 + HV = OH + NO
11.	HO2 + NO2 = HNO2 + O2
12.	HNO2 + OH = H2O + NO2
13.	NO2 + HO2 = HNO4
14.	HNO4 = HO2 + NO2
15.	HO2 + NO = NO2 + OH
16.	RO2 + NO = NO2 + RO
17.	RCO3 + NO + O2 = NO2 + RO2 + CO2
18.	NO2 + OH = HNO3
19.	CO + OH + O2 = HO2 + CO2
20.	O3 + HV = O + O2
21.	HCHO + HV +2 O2 = HO2 + HO2 + CO
22.	HCHO + HV = H2 + CO
23.	HCHO + OH + O2 = HO2 + H2O + CO
24.	RCHO + HV = RO2 + HO2 + CO
25.	RCHO + OH + O2 = RCO3 + H2O
26.	C2H4 + OH = RO2
27.	C2H4 + O = RO2 + HO2
28.	OLE + OH = RO2
29.	OLE + O = RO2 + RCO3
30.	OLE + O3 = (A1)RCHO + (A2)HCHO + (A3)HO2 + (A4)RO2 + (A5)OH + (A6)RO
31.	ALK + OH = RO2
32.	ALK + O = RO2 + OH
33.	ARO + OH = 0.046 DNC + 0.544 RCHO + 0.114 HCHO + 0.05 HNO3 + 0.16 HO2 + 0.84 TOLR
34.	RO = (B1M)RO2 + (B1)HO2 + (B2)HCHO + (B3)RCHO
35.	RONO + HV = NO + RO
36.	RO + NO = RONO
37.	RO + NO2 = RNO3
38.	RO + NO2 = RCHO + HNO2
39.	NO2 + RO2 = RNO4
40.	NO2 + RO2 = RCHO + HNO3
41.	RNO4 = NO2 + RO2
42.	RCO3 + NO2 = PAN
43.	PAN = RCO3 + NO2
44.	NO2 + NO3 = N2O5
45.	N2O5 = NO3 + NO2
46.	H2O + N2O5 = HNO3 + HNO3
47.	O3 + OH = HO2 + O2
48.	O3 + HO2 = OH + O2 + O2
49.	O3 = LOSS
50.	HO2 + HO2 = H2O2 + O2
51.	H2O2 + HV = OH + OH
52.	RO2 + RO2 = RO + RO + O2
53.	NO3 + HCHO + O2 = HNO3 + HO2 + CO
54.	NO3 + RCHO + O2 = HNO3 + RCO3
55.	NO3 + HV = NO2 + O
56.	NO3 + OLE = HNO3 + RCO3
57.	NO2 + NO3 = NO2 + NO + O2

where: RCHO is lumped aldehydes; ALK is lumped alkanes; OLE is lumped olefins; ARO is lumped aromatics; TOLR is toluene radical; DNC is dinitrocresol aerosol; RONO is lumped nitrates; RNO3 is lumped nitrite; RNO4 is lumped peroxy nitrates; RO is alkoxyl radical; RO2 is peroxyalkyl radical RCO3 is peroxyacyl radical; and coefficients A1, A2, A3, A4, A5, A6, B1M, B1, B2, B3 are given in Russell *et al.*, 1988a.

TABLE 2. Summary of Rate Coefficients Used in the Photochemical Box Model.

Reaction No.	Rate coefficient, ($ppmv^{-1}min^{-1}$)	Reference
1.	Varies, solar dependent	
2.	6.E-34*(300./T)**2.3*CNV2	Atkinson *et al.*, 1989
3.	6 1.8E-12*EXP(-1370./T)*CNV1	Atkinson *et al.*, 1992
4.	6.5E-12*EXP(120./T)*CNV1	Atkinson *et al.*, 1992
5.	1.67E5/T*EXP(584./T)	Russell *et al.*, 1988a
6.	1.07E6/T	Russell *et al.*, 1988a
7.	1.2E-13*EXP(-2450./T)*CNV1	Atkinson *et al.*, 1992
8.	1.8E-11*EXP(110./T)*CNV1	Atkinson *et al.*, 1992
9.	5.07E6/T	Russell *et al.*, 1988a
10.	Varies, solar dependent	
11.	17.3/T*EXP(1006./T)	Russell *et al.*, 1988a
12.	1.8E-11*EXP(-390./T)*CNV1	Atkinson *et al.*, 1992
13.	1.73E4/T*EXP(1006./T)	Russell *et al.*, 1988a
14.	1.8E15*EXP(-9950./T)	Russell *et al.*, 1988a
15.	3.7E-12*EXP(240./T)*CNV1	Atkinson *et al.*, 1992
16.	4.2E-12*EXP(180./T)*CNV1	Atkinson *et al.*, 1992
17.	4.2E-12*EXP(180./T)*CNV1	Atkinson *et al.*, 1992
18.	4.53E6/T	Russell *et al.*, 1988a
19.	1.5E-13*(1.+0.6*PATM)*CNV1	Atkinson *et al.*, 1992
20.	Varies, solar dependent	
21.	Varies, solar dependent	
22.	Varies, solar dependent	
23.	8.8E-12*EXP(25./T)*CNV1	Atkinson *et al.*, 1992
24.	Varies, solar dependent	
25.	2.36E4	Russell *et al.*, 1988a
26.	1.2E4	Russell *et al.*, 1988a
27.	1.219E3	Russell *et al.*, 1988a
28.	8.9142E4	Russell *et al.*, 1988a
29.	2.2118E4	Russell *et al.*, 1988a
30.	0.136	Russell *et al.*, 1988a
31.	5.800E3	Russell *et al.*, 1988a
32.	99.8	Russell *et al.*, 1988a
33.	1.6112E4	Russell *et al.*, 1988a
34.	2.0E5	Russell *et al.*, 1988a
35.	4.6*K(10)/4.	McRae, 1981
36.	4.38E6/T	Russell *et al.*, 1988a
37.	2.19E6/T	Russell *et al.*, 1988a
38.	1.91E5/T	Russell *et al.*, 1988a
39.	1.64E6/T	Russell *et al.*, 1988a
40	5.5	Falls and Seinfeld, 1978
41.	1.8E15*EXP(-9950./T)	Russell *et al.*, 1988a
42.	2.05E6/T	Russell *et al.*, 1988a
43.	4.77E16*EXP(-12516./T)	Russell *et al.*, 1988a
44.	2.E-12*(T/300.)**0.2*CNV1	Atkinson *et al.*, 1992
45.	9.7E14*(T/300.)**0.1*EXP(-11080./T)*60.	Atkinson *et al.*, 1992
46.	5.66E-4/T	Russell *et al.*, 1988a
47.	1.9E-12*EXP(-1000./T)*CNV1	Atkinson *et al.*, 1992
48.	1.4E-14*EXP(-600./T)*CNV1	Atkinson *et al.*, 1992
49.	0.	Russell *et al.*, 1988a
50.	2.5E4/T*EXP(1150./T)+5.8E-5* EXP(5800./T)*PPMH2O/T**2	Russell *et al.*, 1988a
51.	Varies, solar dependent	
52.	2.04E4/T*EXP(223./T)	Russell *et al.*, 1988a
53.	0.86	Atkinson *et al.*, 1992
54.	3.6	Atkinson *et al.*, 1992
55.	Varies, solar dependent	
56.	1826.7/T	Russell *et al.*, 1988a
57.	0.59	Russell *et al.*,1988a

where: PATM is atmospheric pressure, in atmospheres; PPMH2O is water vapor concentration, in ppmv; CNV1 is the con-version factor from $molecule^{-1}$ cm^3 s^{-1} to $ppmv^{-1}min^{-1}$ = 4.4E17*(PATM/T); CNV2 is the conversion factor from $molecule^{-2}$ cm^6 s^{-1} to $ppmv^{-2}min^{-1}$ 3.23E33*$(PATM/T)^2$.

TABLE 3. References for Photochemical Absorption Cross Sections and Quantum Yields.

Reaction	Cross-section	Quantum yield
1	Atkinson *et al.*, 1992	Same
10	Atkinson *et al.*, 1992	Same
20	Atkinson *et al.*, 1992	Same
21	Demerjian *et al.*, 1980	Same
22	Demerjian *et al.*, 1980	Same
24	Atkinson *et al.*, 1992	Same
35	0.25 * K(10), McRae Ph.D. thesis, 1981	
51	Demerjian *et al.*, 1980	Same
55	Atkinson *et al.*, 1992	Same

from surface stations prompted us to use the parameterized equations of Reynolds *et al.* (1973) to calculate vertical turbulent diffusivities (K_z, m^2min^{-1}) and wind speeds at all levels:

$$K_z = (2.5q-77.3)\,\rho + 30.9 \text{ for } 0 \le \rho < 0.4$$
$$K_z = q \text{ for } 0.4 \le \rho < 0.8$$
$$K_z = 5(30.9-q)\,\rho + 5q - 123.6 \text{ for } 0.8 \le \rho \le 1.$$

Where $q = 0.85\sqrt{(u^2 + v^2)} + 232$ (m^2min^{-1}); u and v are wind speed components in m min^{-1}; and ρ = (z-h)/H-h); z is height above ground; h is the elevation of the ground at the site of simulation; H is the elevation of the assumed upper level for vertical mixing or transport. To calculate the vertical diffusivity at a chosen level, ground-level altitude, mixing depth, height of the layer, and wind speed at the layer must be known. The mixing depth was taken as the height of the surface inversion during the morning hours. An inversion height of 100 m for summer months (JICA, 1988) was used for the initial mixing depth. The inversion was allowed to rise exponentially, starting at 6:00 AM. The inversion disappeared by 9:00, and the mean maximum mixing depth of 2420 m (Jáuregui *et al.*, 1981; Jáuregui, 1983) was used for the remaining daylight hours. The horizontal diffusivity was set as a constant of 2980 m^2 min^{-1} (Reynolds *et al.* 1973).

Quantification of loss rates by deposition to the ground is difficult. These rates depend on average roughness length, average zero-plane displacement length, and depth of the roughness sublayer (Oke *et al.*, 1992). Table 4 summarizes the deposition velocities used in the model.

TABLE 4. Deposition Velocities Used in the Box Model.

Species	Deposition velocity (mm^{-1})	Reference
NO	0.12	Hicks, 1984
NO2	1.0	Hicks, 1984
O3	3.8	Hicks, 1984
HCHO	0.55	McRae *et al.*, 1982
RCHO	0.09	McRae *et al.*, 1982
H2O2	0.55	McRae *et al.*, 1982
PAN	0.18	Hicks, 1984
HNO3	1.74	McRae *et al.*, 1982
NH3	0.18	McRae *et al.*, 1982
NIT	0.09	McRae *et al.*, 1982

4. Initial concentrations

The initial concentrations of most "criteria" pollutants were taken from data collected at the surface monitoring station at the headquarters of the Mexican Meteorological Service at Tacubaya Observatory. The data reported for midnight provided some initial species concentrations: NO=3, NO_2=30, O_3=25, CO=2700 ppbv. Initial concentrations for reactive hydrocarbons are more difficult to obtain since, although some stations report non-methane hydrocarbon concentrations, they do not report individual hydrocarbon species. In order to obtain a "snapshot" of hydrocarbon speciation, air samples were collected at seven separate sites in Mexico City (Fig. 2) on November 29 and November 30, 1993. Sampling occurred between the hours of 8:00 and 11:00 Local Standard Time on both days. A 1.5-volt battery-operated pump drew known volumes of air through thermal desorption tubes (Supelco, Carbotrap 300). The meteorological conditions were similar on both days. Winds came from the north or northwest at 2 to 8 ms^{-1} for much of the two days. Temperatures ranged from 6 to 22 C with little cloud cover. Relative humidity ranged from 65% at 7:00 to 20% in the late afternoon.

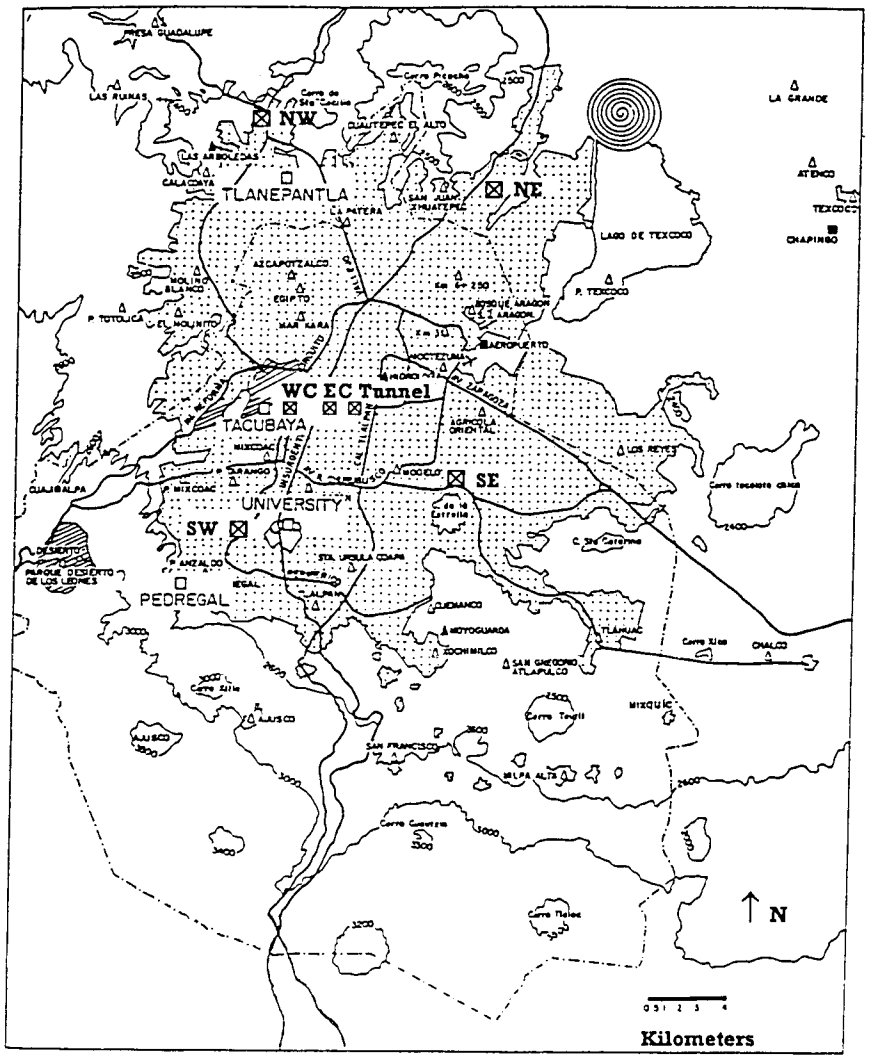

Fig. 2. Map of air sampling sites (Jáuregui, 1988).

The Carbotrap samples were thermally desorbed and analyzed for hydrocarbons at the Mass Spectrometry Facility at the University of Arizona (Table 5). The samples of November 29 were analyzed for low molecular weight hydrocarbons, while those of November 30 were analyzed for heavier species. Measured propane and butane levels were significantly higher than ethane levels, with butane levels approximately one-third that of propane. This unusual relative distribution has recently been ascribed to leaks of liquified petroleum gas (Baum, 1995). Olefin concentrations (excluding ethene) appear to be significantly higher than typically found in U.S. cities (National Research Council, 1991). The ethene values may be too low, as the thermal desorption tube is designed to trap $\geq$ C5 species (Supelco Carbotrap 300 data sheet). Therefore it is possible that some ethene was lost during sample shipment. Initial concentrations for this species were based on typical Los Angeles values (California E.P.A. Air Resources Board, 1992). Aldehyde concentrations were taken from Bravo *et al.* (1991).

TABLE 5. Concentrations of Hydrocarbons (ppbv), Measured at Seven Sites in Mexico City on November 29 and November 30, 1993.

Sector	NW	NE	WC	EC	SW	SE	Tunnel
ethene			35	14			
propene	36	28		51			54
propane	180	220	67	220	5	284	320
butane	74	75	36	94		121	180
1-pentene	50	190	31	120			135
pentane	48		9	77		64	110
benzene	9	4	11	13	3	14	35
toluene	27	61	18	68	9	85	50
p-dichloro-benzene	3	5	6	190	1	12	0
xylenes	24	61	110	110	12	121	99
C3 substituted benzenes	47	74	130	240	14	114	110

The hydrocarbon data were lumped into four categories to match those used in the model. The lumped values (Table 6) provided estimates of the initial speciated hydrocarbon concentrations needed to initialize the model. Values from the SW and SE samples were not used in the averaging process because of suspected sampling errors, indicated by abnormally low olefin concentrations. The alkane result for the Tunnel sample and the aromatic result from the East Central sample were similarly discarded from the averaging process since they appeared to be anomalously high. From the above information, speciated hydrocarbon concentrations for model initialization at 00:00 were estimated as: alkanes=275, ethene=100, olefins=139, aromatics=221, formaldehyde=10, higher aldehydes=7 ppbv. These data agree reasonably well with the reported typical background concentration of non-methane hydrocarbon of 600 ppbv (JICA, 1988). Although this hydrocarbon speciation data are very limited, it appears that there is a higher than normal proportion of ethene and olefins in the MCMA air.

The other major species requiring an initial value was peroxyacetyl nitrate (PAN). It is not regularly monitored in the MCMA. An initial value was obtained by running the model with no initial PAN for a 24 hour simulation. The resulting 24:00 value (7 ppbv) was then used as the 00:00 value for further modeling

simulations. This concentration is comparable to the 4 ppbv value used to initialize the model in a study of pollution in the Los Angeles air basin (Russell et al., 1988a). Measured peak values of PAN in that study ranged between 9 to 17 ppbv, depending on site and day of measurement.

TABLE 6. Lumped hydrocarbon concentrations (ppbv).

Sector	NW	NE	WC	EC	SW	SE	Tunnel
ethene			35	14			
alkanes	302	295	112	391	5	469	610
olefins	86	218	31	171	0	0	189
aromatics	110	205	275	621	39	346	294

Following the procedure in Russell *et al.* (1988a), initial ozone concentrations for the second layer were set as the ground-level concentration at 14:00 of the previous day. Initial concentrations of all other species in this layer were set at zero. Initial species concentrations at all other layers were set at zero.

5. Emissions data and meteorology

Emissions data for nitrogen dioxide, carbon monoxide, and hydrocarbons were based primarily on the JICA Report (1988), where sources of these pollutants from automobiles, jet airplanes, factories, and service and commercial establishments in the Federal District were calculated. Hourly automobile emissions are summarized in Table 7 (JICA, 1988). The line sources are from major roads while area sources are estimates over less travelled roads. A summary of source emissions for the MCMA is listed in Table 8 (JICA, 1988). These emissions are reported as daily averages. Urban splitting factors (Russell *et al.*, 1988a) were used to speciate the total hydrocarbon source report in Table 7 to use the lumped kinetics in the computer model. The factors and corresponding emissions for MCMA are given in Table 9.

TABLE 7. Hourly pollutant emission rate (24h average) for automobiles (Nm^3h^{-1}).

Vehicle Class		Passenger Car	Bus	Truck	Combi	Total
Source						
	CO	30768	242	11308	3403	45721
Line	NOx	623	242	150	99	1114
	HC	3969	297	1568	703	6537
Area	CO	31941	320	12716	5208	50185
	NOx	606	315	132	126	1179
	HC	4367	402	1830	1122	7721
	CO	62709	562	24024	8611	95906
Total	NOx	1229	557	282	225	2293
	HC	8336	699	3398	1825	14258

These estimates of hydrocarbon emissions appear to give reasonable concentrations for Mexico City. The volume of air used to calculate net hydrocarbon emissions was the area of the modeled region multiplied by the mixing height, as a function of time. These emissions produce a non-methane hydrocarbon concentration of 3.5 ppmv. When these emissions are added to the background non-methane hydrocarbon concentration of 0.75 ppmv used to initialize the lumped hydrocarbon species in the model,

the resulting non-methane hydrocarbon concentration of 4.25 ppmv compares favorably with the peak measurement of 4.5 ppmv cited by Ruiz-Suárez (1989). The CO source emissions were assumed to be as solely due to automobiles.

TABLE 8. Pollutant emissions by source; 24h average (Nm^3h^{-1}).

Class	Sources	CO	NO_x
Stationary Sources	Power plants		801.9
	March 18 Refinery		214.8
	Other factories		284.1
	Service & Commercial		50.9
Mobile Sources	Automobiles	95906	2293.0
	Airplanes		10.5
Total		95906	3655.2

TABLE 9. Hydrocarbon emissions by class.

Species	Urban Splitting Factor	Emission (Nm^3h^{-1})
HCHO	0.0037	52.75
RHCO	0.0033	47.05
OLE	0.0042	59.88
ALK	0.0675	962.42
ARO	0.0177	252.37
C2H4	0.0061	86.97

TABLE 10. NO emissions.

Source	NO factor	Emission (Nm^3h^{-1}).
Automobiles	0.99	2269.7
Power plants	0.95	761.8
Aircraft	0.99	10.4
Other fixed sources	0.98	538.8
Total		3580.7

The NO_x emissions were split between NO and NO_2 using the splitting factors of Roth *et al.* (1974). They are summarized in Table 10. Using the data in Table 10 gives total NO emissions of 3582 Nm^3h^{-1} while the total NO_2 emissions are estimated as 74 Nm^3h^{-1}.

Hourly meteorological data from the Tacubaya Observatory necessary to run the model included temperature, air pressure and relative humidity profiles, and wind speed.

6. Base case

A base case model run using the listed initial conditions was used to compare predicted pollutant concentrations to measured concentrations. The model calculated changes in concentrations at each time step through a three-part process. First, the coupled differential continuity equations were solved using concentrations determined from the previous time step. Second, pollutant emissions were added to the modeled region. Since vehicles are the major source of emissions, this addition strongly reflected the morning and evening rush hours. The sources were added between 6:00 to 9:00 Local Standard Time and again between 18:00 and 20:00. The emissions were treated as an area source for all simulations, as they were added to the ground layer of the modeling region without bias towards a specific location. Third, pollutant gain and loss through transport and deposition was estimated.

Reactive hydrocarbons, NO_x, and carbon monoxide were added steadily at the onset of rush hours, until the total emission values were reached. The emissions were reduced gradually at the end of rush hours.

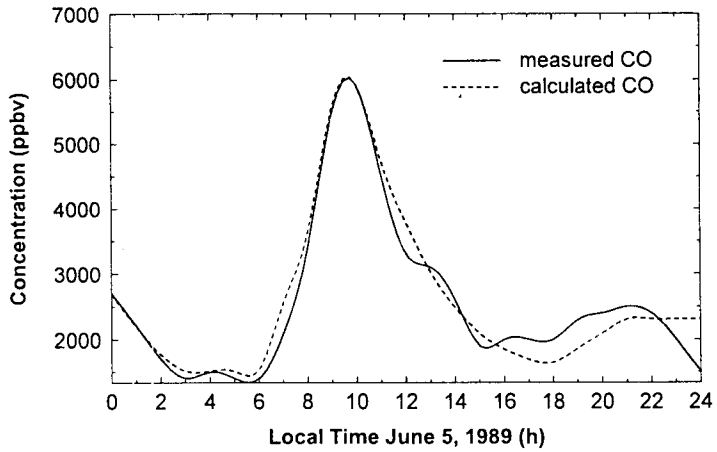

Fig. 3. Measured and calculated CO concentration profiles for the base case model run.

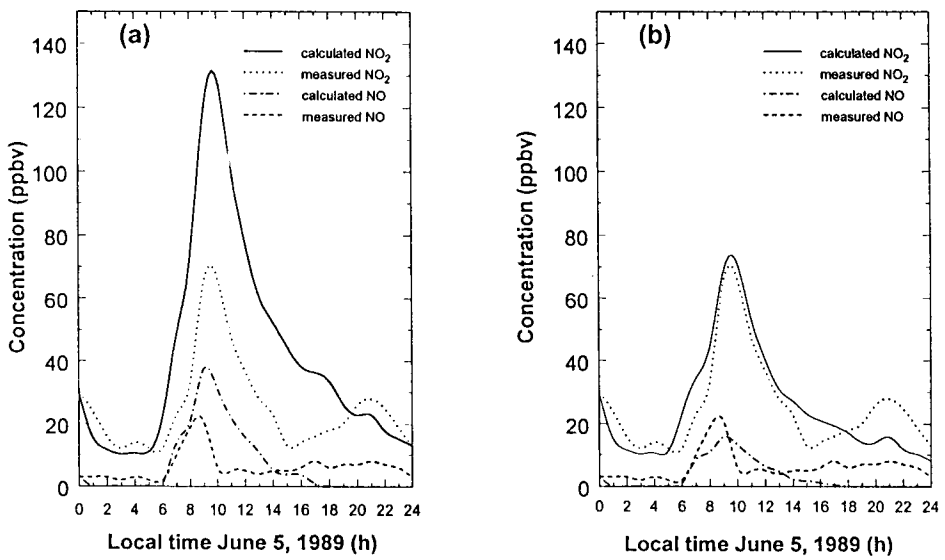

Fig. 4. (a) Measured and calculated NO and NO_2 concentration profiles for the base case. Calculated values were derived from the emissions inventories in JICA (1988); (b) NO_x profile calculated from a 50% reduction in JICA (1988) estimates.

Carbon monoxide is relatively inert and therefore it was assumed that to a first approximation the predicted CO profile would follow the measured profile. Consequently, calculated CO emission rates at the beginning and end of rush hours were "calibrated" to match the measured profile (Fig. 3). The base case was completed by adjusting emission rates for all sources of all primary pollutants to correspond to the CO "calibration". The calculated and measured concentration profiles for NO_x are presented in Figure 4, while those for ozone are presented in Figure 5. It can be seen that the times of the predicted NO_x and O_3 peaks match those of the measured peaks, and the predicted ozone peak value of 154 ppbv closely matches the measured value of 158 ppbv (Fig. 5a). However, the predicted maximum NO and NO_2 levels are about double the measured levels (Fig. 4a).

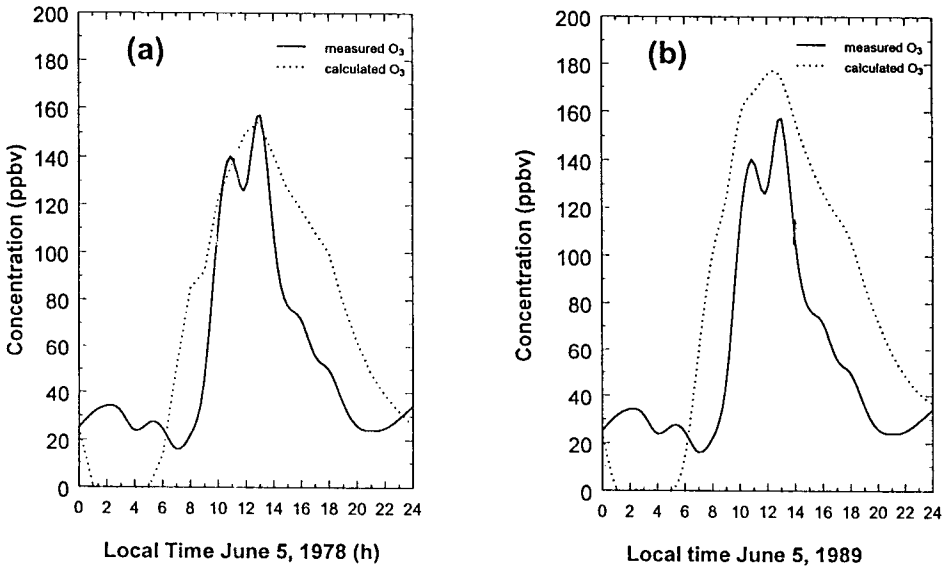

Fig. 5. (a) Measured and calculated O_3 concentration profiles for the base case; (b) O_3 profile calculated for a 50% reduction in NO_x emissions.

The reason for the NO and NO_2 discrepancies is not known but is probably associated with the emissions inventory or the splitting factor. Comparison of the Tacubaya NO_x measured profile with NO_x profiles measured in other areas in the MCMA show good agreement, and therefore the measurements are probably correct. This implies that the NO_x emissions inventory estimated by JICA (1988) may be too large by a factor of approximately 2. If the estimated NO_x emission rate is reduced by 50% then the agreement between calculated and measured NO and NO_2 profiles is much better (Fig. 4b). Under the 50% NO_x conditions, the calculated peak O_3 levels actually increase 15% from 154 to 177 ppbv (Fig. 5b) probably due to lower consumption of O_3 by NO.

7. Results and discussion

Ozone isopleths (Fig. 6) were calculated by systematically varying the initial NO_x and lumped reactive hydrocarbons with respect to the base case. All other conditions remained the same. The lumped reactive hydrocarbons, i.e. alkanes, ethene, olefins, and aromatics, were varied as a group while maintaining the

original hydrocarbon splitting factors. The ozone isopleths (Fig. 6) show that O_3 in the MCMA may be hydrocarbon-limited (for the assumed case conditions) and consequently that large variations in NO_x levels would have relatively little affect on O_3 production. This is contrary to what we would have been expected for the hydrocarbon-rich atmosphere of Mexico City (Ruiz *et al.*, 1996) and indicates that the emissions inventory may be erroneous.

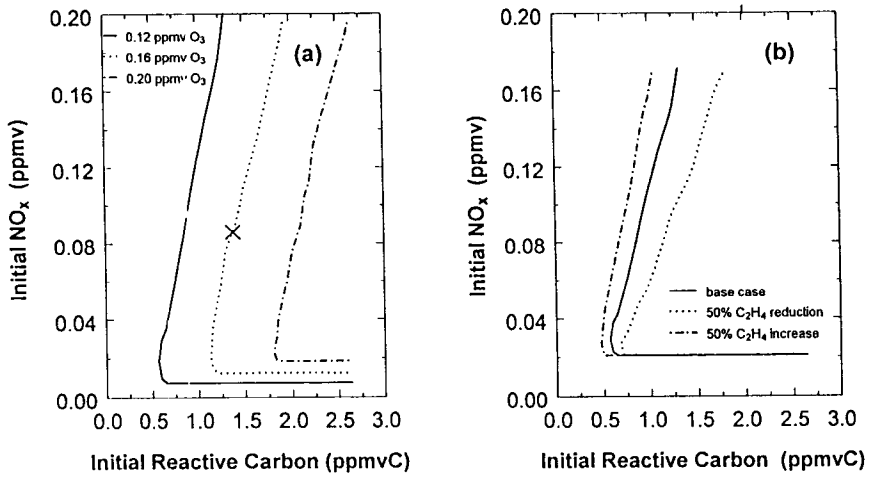

Fig. 6. (a) Ozone isopleths calculated for the base case. The MCMA is located at the point marked "X" ; (b) Effect of varying ethene levels by +- 50% on the position of the 0.12 ppmv O_3 isopleths.

Sensitivity to hydrocarbon splitting factors was studied by varying the emissions of each individual class in the base case. Four more ozone isopleth plots (not shown here) were created by running the model for separately increased alkane, ethene, olefin, or aromatic emissions. In these model runs, the emission for one class was increased by 20%, while all other initial base case data remained the same. Similarly, four additional isopleth plots (not shown here) were made with 50% decrease in emissions by hydrocarbon class. There was minimal shifting of the isopleths to the left or right, with no discernible change of slopes (compared to Fig. 6) in most cases. Only in the cases involving ethene were there marked differences (Fig. 6b). The MCMA appears to be characterized by exceptionally high levels of olefins and aromatics compared to a U.S. "all-city average" (National Research Council, 1991) which may account for the compression of the O_3 ridge near the bottom of the isopleth (Fig. 6a). A highly reactive hydrocarbon mix in a hydrocarbon-limited atmosphere would be expected to steepen the vertical leg of the isopleth. This can be seen in Figure 6b where the effects of ethene levels were calculated.

The preliminary ozone isopleths for Mexico City generated by this multi-layer box model indicate that reduction of reactive organic carbon (ROC) would be the most efficient method to lower ozone concentrations. However, the ROC would need to be reduced to approximately 50% of the modeled levels before reaching the standard of 0.12 ppmv O_3. It should be noted that this conclusion is highly dependent on the validity of the assumed ROC and NO_x inventory. The MCMA ROC/NO_x ratio is approximately 15 in this study which places it mid-way between generally accepted criteria for ROC control (ROC/NO_x ~ $\leq$ 10) and for NO_x control (ROC/NO_x ~ $\leq$ 20) (National Research Council, 1991). If the NO_x inventory estimates are indeed too high by a factor of 2 (see above) then the MCMA ROC/NO_x $\approx$ 30 and NO_x control

strategies would be indicated. The Mexico City Air Quality Research Initiative (MARI), a joint effort between the U.S. Department of Energy Los Alamos Laboratory and the Instituto Mexicano del Petróleo (IMP) (MARI, 1996) concludes that the MCMA O_3 is probably NO_x-limited but that ROC controls should nevertheless be implemented for other reasons.

The isopleths calculated for our assumed conditions also suggest that decreases in NO_x emissions would have little immediate effect on ozone levels if hydrocarbon levels remained unaltered. A simultaneous reduction of hydrocarbon and NO_x emissions in which the present ROC/NO_x ratio was maintained would also have little immediate effect on O_3 levels. However, these preliminary conclusions should be interpreted cautiously considering the possible erroneous emissions inventory. Historically, many model simulations may have relied on emissions inventories that underestimate reactive hydrocarbons (National Research Council, 1991). Resulting analyses would tend to overestimate the effectiveness hydrocarbon control measures and underestimate the effectiveness of NO_x controls. Also, while a NO_x or reactive hydrocarbon reduction scheme may decrease ozone in the metropolis, there could be significant ozone increases downwind.

Emissions for this study reflect values from 1988 inventories (the latest data available). Possible emission reductions since then have not been taken into account. For example, a government oil refinery was closed in March, 1991, i.e., 3 years after the emissions inventories were estimated. The refinery contributed approximately 6% of the NO_x emissions (Table 8). However, when these emissions were omitted from a modified base case run, there was no significant effect on the ozone isopleths.

There are limitations to the modeling study reported here. As noted in the introductory section, a box model cannot be applied confidently if the airshed pollutant concentrations are not homogeneously distributed or the meteorology is complex. Much of the industrial pollution is generated in the northeastern part of the MCMA and is advected by winds from the north or northwest. Jáuregui (1973; 1986; 1988) has indicated that the urban heat island effect can create complex wind patterns which have a strong influence on pollution.

The physical conditions of Mexico City may limit the effectiveness of existing chemical mechanisms in pollutant prediction (Ruiz-Suárez, 1989; Ruiz-Suárez *et al.*, 1993). The combination of lower atmospheric pressure and increased solar radiation may have a significant influence in calculated pollutant concentrations. Finally, the chemical mechanism used here does not account for sulphur dioxide chemistry or particulates, which are a concern in the MCMA.

Measurement of vertical profiles of pollutant concentrations would help in initializing the model and increase the accuracy of vertical transport estimates. Including a vertical wind profile would aid in determining more accurate vertical turbulent diffusivity values with respect to height. Measured mixing depths would provide a more accurate accounting of emissions.

Most importantly, a systemized monitoring of non-methane hydrocarbon concentrations around the MCMA is needed. As studies of air pollution in Los Angeles (McRae *et al.*, 1983; Russell *et al.*, 1988a; Russell *et al.*, 1988b) indicate, accurate emissions inventories and speciated hydrocarbon concentrations are critical in determining ozone reduction strategies.

Acknowledgements
We are grateful to Daniel Jacob, Harvard University, for providing the initial computer code; to Ernesto Jáuregui, UNAM, Mexico, for providing meteorological data and for useful discussions; to the Dirección General de Ecología, Dirección de la RAMA, DDF for meteorological data; to Marcia Dodge for helpful discussions on ozone isopleths; to R. Quijano of the Programa Universitario de Medio Ambiente at UNAM who coordinated the air sampling efforts; to the Coordinación General de Reordenación Urbana y Protección Ecología; and to Javier Tejeda Ruíz and María Esther Ruíz, IMP, México, for helpful discussions. We also thank Mark Malcomson who performed the GC/MS analysis; and Dean Carter, University of Arizona and the National Institute of Environmental Health Sciences, NIH (ES04940) for partial financial support.

REFERENCES

Atkinson, R., D. L. Baulch, R. A. Cox, R. F. Hampson Jr., J. A. Kerr, and J. Troe, 1989. Evaluated kinetic and photochemical data for atmospheric chemistry: Supplement III. *J. Phys. Chem.* Ref. Data 18, 881-1097.

Atkinson, R., D. L. Baulch, R. A. Cox, R. F. Hampson Jr., J. A. Kerr, and J. Troe, 1992. Evaluated kinetic and photochemical data for atmospheric chemistry: Supplement IV. *Atmos. Environ.* **26**, 1187-1230.

Baum, R., 1995. New source of smog detected in Mexico City. Chem. and Engineering News, April 10, 8.

Bravo, H. A., R. Camacho C., G. Roy Ocotla, R. Sosa E. and R. Torres J., 1991. Analysis of the change in atmospheric urban formaldehyde and photochemistry activity as a result of using methyl-t-butyl-ether (mtbe) as an additive in gasolines of the metropolitan area of Mexico City. *Atmos. Environ.* **25**, 285-288.

California E.P.A. Air Resources Board, 1992. California air quality data, 24, No. 4, 71.

Castro, T., L. G. Ruíz-Suárez, C. Gay, M. Helguera, and J. C. Ruíz-Suárez, 1996. Direct measurements of NO_2 photolysis rates for Mexico City. *Atmósfera* **8**, 137-142.

Coordinación General de Reordenación Urbana y Protección Ecológica, 1991. Reporte de calidad del aire en el primer semestre Ciudad de México, July, 1991. Dirección de Planeación Ecológica.

Demerjian, K. L., K. L. Schere, and J. T. Peterson, 1980. Theoretical estimates of actinic (spherically integrated) flux and photolytic rate constants of atmospheric species in the lower troposphere. *Adv. Environ. Technol.* **10**, 369-459.

Dunker, A. M., S. Kumar, and P. H. Berzins, 1984. A comparison of chemical mechanisms used in atmospheric models. *Atmos. Environ.* **18**, 311-321.

Falls, A. H. and J. H. Seinfeld, 1978. Continued development of a kinetic mechanism for photochemical smog. *Environ. Sci. Technol.* **12,** 1398-1406.

García, E. G., 1977. La Ciudad de México en cifras. Rev. Comercio 19, 12-13.

Harley, R. A., A. G. Russell, G. J. McRae, G. R. Cass, and J. H. Seinfeld, 1993. Photochemical modeling of the Southern California air quality study. *Environ. Sci. Technol.* **27,** 378-388.

Hicks, B. B. (ed.), 1984. Deposition both wet and dry. Butterworth Publishers, 153-193.

Intergovernmental Technical Secretariat, 1991. Comprehensive pollution control program for the Mexico City Metropolitan Zone, April, 1991 revision, 11.

Jáuregui, E., 1971. Mesomicroclima de la Ciudad de México. Universidad Nacional Autóma de México, 87.

Jáuregui, E., 1973. The urban climate of Mexico City. *Erdkunde*, **27**, 298-307.

Jáuregui, E., D. Klaus, and W. Lauer, 1981. Una primera estimación del transporte de SO_2 sobre la Ciudad de México. *Geofísica Internacional,* **20**, 55-79.

Jáuregui, E., 1983. Visibility trends in Mexico City. *Erdkunde* **37**, 296-299.

Jáuregui, E., 1986. The urban climate of Mexico City, in proceedings of WMO technol. conference, T. R. Oke (ed) WMO No. 652, 63-86, Geneva.

Jáuregui, E., 1988. Local wind and air pollution interaction in the Mexico basin. *Atmósfera,* **1**, 131-140.

Japan International Cooperation Agency, 1988. The study on air pollution control plan in the Federal District.

MARI, 1996. Mexico City Air Quality Research Initiative, Final Report, Vol 1-5; Los Alamos National Laboratory DOE contract W-7405-Eng-36.

McRae, G. J., 1981. Mathematical modeling of photochemical air pollution, Ph.D. thesis. California Institute of Technology.

McRae, G. J., W. R. Goodin, and J. H. Seinfeld, 1982. Development of a second-generation mathematical model for urban air pollution--I. Model formulation. *Atmos. Environ.* **16**, 679-696.

McRae, G. J., and J. H. Seinfeld, 1983. Development of a second-generation mathematical model for urban air pollution--II. Evaluation of model performance. *Atmos. Environ.* **17**, 501-522.

National Research Council, 1991. Rethinking the ozone problem in urban and regional air pollution, 351-377. National Academy Press.

Oke, T. R., G. Zeuner, and E. Jáuregui, 1992. The surface energy balance in Mexico City. *Atmos. Environ.* **26**, 433-444.

Reynolds, S. D., P. M. Roth, and J. H. Seinfeld, 1973. Mathematical modeling of photochemical air pollution--I. Formulation of the model. *Atmos. Environ.* **7**, 1033-1061.

Roth, P. M., P. J. W. Roberts, M. Liu, S. D. Reynolds, and J. H. Seinfeld, 1974. Mathematical modeling of photochemical air pollution--II. A model and inventory of pollutant emissions. *Atmos. Environ.* **8**, 97-130.

Ruiz, M. E., J. L. Arriaga and I. García, 1996. Determinación de compuestos orgánicos volátiles en la atmósfera de la Ciudad de México mediante el uso de sistemas ópticos y métodos convencionales. *Atmósfera,* **9**, 119-135.

Ruiz-Suárez, L. G., 1989. Photo-oxidation of hydrocarbons in Mexico City: Effects of altitude. Part 1. *Atmósfera, 2*, 47-63.

Ruiz-Suárez, L. G., T. Castro, B. Mar, M. E. Ruiz-Santoyo, and X. Cruz, 1993. Do we need an *ad hoc* chemical mechanism for Mexico City's photochemical smog? *Atmos. Environ.* **27**, 405-425.

Russell, A. G., K. F. McCue, and G. R. Cass, 1988a. Mathematical modeling of the formation of nitrogen-containing air pollutants. 1. Evaluation of an eulerian photochemical model. *Environ. Sci. Technol.* **22**, 263-271.

Russell, A. G., K. F. McCue, and G. R. Cass, 1988b. Mathematical modeling of the formation of nitrogen-containing air pollutants. 2. Evaluation of the effect of emission controls. *Environ. Sci. Technol.* **22**, 1336-1347.

Seinfeld, J. H., 1986. Atmospheric chemistry and physics of air pollution. John Wiley & Sons.

Supelco, 1992. Carbotrap 300 multi-bed thermal desorption tubes data sheet.

Young, T. R. and J. P. Boris, 1977. A numerical technique for solving stiff ordinary differential equations associated with the chemical kinetics of reactive flow problems. *J. Phys. Chem.* **81**, 2424-2427.